

Published in final edited form as:

Surgery. 2011 December ; 150(6): 1186–1193. doi:10.1016/j.surg.2011.09.026.

Comparison of clinical and imaging features in succinate dehydrogenase-positive versus sporadic paragangliomas

Aradhana M. Venkatesan, MD^a, Hari Trivedi, BS^a, Karen T. Adams, CRNP^b, Electron Kebebew, MD^c, Karel Pacak, MD, PhD, DSc^b, and Marybeth S. Hughes, MD^c

^aCenter for Interventional Oncology, Radiology and Imaging Sciences, National Institutes of Health, Bethesda, MD

^bSection on Medical Neuroendocrinology, Eunice Kennedy Shriver National Institute of Child Health and Human Development, Bethesda, MD

^cEndocrine Oncology Section, Surgery Branch, National Cancer Institute, Bethesda, MD

Abstract

Background—Limited data exist concerning the clinical and imaging features that distinguish sporadic from familial paragangliomas (PGLs).

Methods—Clinical, genetic (succinate dehydrogenase [*SDHB*] vs no SDHx), and imaging (computed tomography [CT], magnetic resonance imaging, ¹⁸F-fluoro-deoxy-glucose positron emission tomography [¹⁸F-FDG-PET]) features obtained during a decade in 124 PGL patients were studied. Data were analyzed by Fisher’s exact test or Wilcoxon rank-sum test.

Results—Mean age at diagnosis was younger in the *SDHB*-positive (*SDHB*+) group compared with the sporadic (no SDHx) group (28 vs 39 years, respectively, $P < .001$). Rate of supradiaphragmatic neoplasms were greater in the *SDHB*+ group (16.7 vs 4.7%, $P = .11$). Metastasis rates were greater in the *SDHB*+ group (78.9 vs 48.3%, $P < .001$), as was the existence of metastases or multiple PGLs at presentation (38.5 vs 16.7%, $P < .05$). Tumor volumes >250 mL were exclusively observed in *SDHB*+ patients ($P < .05$). On CT, *SDHB*+ tumors were more enhanced ($P < .05$). On ¹⁸F-FDG-PET, *SDHB*+ tumors’ had greater mean standard uptake values (12.3 vs 8.0, $P < .05$).

Conclusion—Clinically young age, large tumor volume, greater rate of metastatic and multifocal PGLs, greater SUV values on ¹⁸F-FDG-PET, and increased CT enhancement are observed in *SDHB*+ PGLs. These findings may warrant genetic screening. Because *SDHB*+ patients demonstrate more supradia-phragmatic lesions, whole-body imaging may be of particular value in these patients.

Paragangliomas (PGLs) are tumors derived from sympathetic chromaffin tissue in adrenal and extra-adrenal abdominal, pelvic, or thoracic locations, or from parasympathetic tissue of the head and neck.¹ PGLs arising from the adrenal medulla are referred to as pheochromocytomas.^{2,3} PGLs can develop sporadically or in familial genetic conditions.⁴⁻⁷ Several genes implicated in the pathogenesis of hereditary PGL have been recently described.⁴⁻⁷ Mutations in genes encoding the B, C, and D subunits of the mitochondrial complex II enzyme succinate dehydrogenase (*SDHB*, *SDHC*, and *SDHD*, respectively) are each associated with a distinct clinical syndrome.⁸⁻¹¹ Aggressive familial PGLs are most

commonly the result of germline B subunit mutations in the succinate dehydrogenase (*SDHB*) gene, with *SDHB*-related PGLs predominantly occurring in extra-adrenal abdominal or thoracic locations and with up to 70% being malignant.^{8–11}

However, limited data are available concerning clinical and imaging features that may distinguish sporadic from this particular category of familial PGLs, thereby prompting genetic screening when appropriate.^{8–11} The aim of this study was to evaluate the clinical, genetic, and imaging features of 124 patients with histologically confirmed PGLs, including 61 patients with known *SDHB* germline mutation and 63 patients with no mutation known to result in familial PGL. Mean age at diagnosis, type of clinical presentation, rate of supra- and infra-diaphragmatic neoplasms, metastatic disease rates, incidence of metastases or multiple PGLs at presentation, overall recurrence rates, median tumor volume, T2-weighted appearance on magnetic resonance imaging (MRI), enhancement characteristics on computed tomography (CT), and ¹⁸F-fluoro-deoxy-glucose positron emission tomography (¹⁸F-FDG-PET) activity were compared between these two groups.

METHODS

Patients

A total of 61 patients (41 male, 20 female) with an *SDHB* mutation were included in this retrospective study; in addition, 63 patients (42 male, 21 female) who were genetically tested and had no known *SDHB*, *SDHx*, or any other genetic predisposition and who had a histologically proven abdominal or thoracic PGL also were included in this study and, because of a lack of known genetic risk, were deemed sporadic cases. All patients were referred to the National Institutes of Health (NIH) for a consultation regarding an optimal treatment plan for (suspected) metastatic PGL between August of 2000 and February of 2011. The study protocol was approved by the institutional review board of the National Institutes of Child Health and Human Development at the NIH. All patients provided written informed consent for all genetic, biochemical, and imaging studies regarding PGL. Genetic testing was performed at the Department of Human Genetics of the Pittsburgh University Medical Center as described elsewhere.¹²

Clinical data

Patient age at diagnosis and time to diagnosis from initial symptom onset was recorded for both *SDHB*+ and sporadic patients. The type of clinical presentation was also recorded for each group. Acute presentation was defined as sudden signs or symptoms of hypertension, tachycardia, syncope, or acute pain. If tumors were detected on cross-sectional imaging performed for screening purposes and in the absence of clinical history signs and symptoms of catecholamine excess, they were classified as incidentally detected. The type of presentation was unavailable or unclear from clinical history in 5 *SDHB*+ patients and 15 sporadic patients. Tumor location, including supra- and infra-diaphragmatic location, was recorded in 54 *SDHB*+ patients and 42 sporadic patients. The rate of metastatic disease, multifocal disease, and tumor recurrence was recorded, including occurrences before presentation or during the course of follow-up at the NIH in 57 *SDHB* and 60 sporadic patients.

Imaging methods

CT, MRI, and ¹⁸F-FDG-PET imaging that delineated patients' PGLs were available for only a subset of the *SDHB*+ and sporadic patients because many patients underwent surgical resection before being referred to the National Institutes of Health. CT scans of the neck, chest, abdomen, and pelvis were performed between August 2000 and February 2011 with a variety of equipment, including LightSpeed Ultra, LightSpeed QX/i, HiSpeed CT/i, Genesis

Hi-Speed (General Electric Healthcare Technologies, Waukesha, WI), and M_8000 IDT (Philips Medical Systems, Andover, MA) scanners. CT scans of tumor were available in 27 *SDHB+* and 25 sporadic patients. Section thickness was up to 3 mm in the neck and 5–10 mm through the chest, abdomen, and pelvis. All studies except one were performed with a rapid infusion of non-ionic water-soluble intravenous contrast agent, given when feasible, as well as oral contrast material.

MRI of the neck, chest, abdomen, and pelvis was obtained with 1.5- or 3-Tesla scanners (General Electric Healthcare Technologies and Philips Medical Systems, respectively). Phased-array coils were used for neck imaging, and either phased-array torso or quadrature body coils elsewhere. MRI of tumors was available in 21 *SDHB+* and 23 sporadic patients. T1-weighted gradient-echo, and short-tau inversion recovery and/or fat-suppressed fast spinecho T2-weighted imaging parameters were adjusted so as to minimize examination time while achieving desired anatomic coverage. Image slice thickness was 3–10 mm. Preinjection images were obtained in the axial plane. Contrast-enhanced images were obtained after injection of a gadolinium-diethylenetriamine pentaacetic acid contrast agent by the use of fat-suppressed T1-weighted gradient-echo imaging, generally in both axial and coronal planes.

For ^{18}F -FDG-PET imaging, patients fasted for 6 hours before intravenous injection of FDG (Cardinal Health, Beltsville, MD) and refrained from caffeine, tobacco, and alcohol for 12 hours. All ^{18}F -FDG scans were performed by use of a Discovery ST PET/CT scanner (General Electric Medical Systems). Patients were imaged supine from head to proximal thighs (slice 128×128 matrix; voxel size $4.24 \text{ mm} \times 4.25 \text{ mm} \times 3.27 \text{ mm}$). For 18 *SDHB+* and 23 sporadic patients, CT was followed by ^{18}F -FDG-PET, acquired during shallow respiration without oral or intravenous contrast (120 kVp, 115 mA, and 20 mm [16×1.25 mm] collimation). CT images (3.75-mm thick, 512×512 slices) were used for anatomic co-registration and PET attenuation correction. PET images, originally expressed in activity concentration (Bq ml^{-1}), were rescaled to represent standardized uptake value (SUV). Maximum SUV in the image of the lesion (SUV_{max}) was used as an indicator of lesion metabolic activity.

Image analysis

All imaging data were reviewed by a radiologist (AV) who was blinded to patient mutational status and clinical data at the time of image interpretation and analysis. CTs were evaluated to identify the primary tumor's location and size and to confirm the presence of multifocal disease or metastatic disease. The volume of the primary tumor was calculated by use of the formula for the volume of a prolate ellipsoid ($\pi/6 \times D1 \times D2 \times D3$, with D1, D2, and D3 representing tumor diameter in the x, y, and z planes, respectively). CT enhancement of tumors was measured by drawing maximal regions of interest around the margins of the primary tumor on the postcontrast images obtained, which were largely studies performed during the portal venous phase of enhancement. These CT densities, in Hounsfield units (HU), were recorded. MRIs were reviewed to determine the appearance and MR characteristics of the primary tumor. T2-weighted appearances were classified by the use of a four-point classification system as described by Jacques et al.¹³ ^{18}F -FDG-PET images were evaluated to determine whether the primary tumor was FDG-avid. FDG-avidity was defined as uptake of FDG that was greater than background uptake within soft tissue and muscle. Maximum SUV were selected on the image of the lesion (SUV_{max}) and used as an indicator of lesion metabolic activity.

In cases in which patients presented with multifocal or multiple metastatic tumors on their CT, MRI, and ^{18}F -FDG-PET scans (10 sporadic patients, 20 *SDHB+* patients), the largest tumor evident on these scans was selected and its CT HU density, MRI T2 signal, and

SUV_{max} were calculated with the use of the same methodology as described for patients with solitary tumors.

Statistical methods

Clinical and imaging features between the *SDHB*⁺ and sporadic groups were compared by the use of Fisher's exact test for categorical variables (presentation type, clinical outcomes, MRI classification, tumor location) and Wilcoxon rank-sum test for continuous variables (age at diagnosis, time to diagnosis, tumor volumes, CT enhancement, and SUV uptake).

RESULTS

Clinical data for *SDHB*⁺ versus sporadic patients is summarized in Table I. Mean age at diagnosis was lower in the *SDHB*⁺ group (28 ± 15 years) compared with the sporadic group (39 ± 14 years, $P < .001$). The greatest number of *SDHB*⁺ patients presented in the first 4 decades compared with a majority of presentations in the 4th-6th decades in the sporadic group (Fig 1). There was no significant difference in time to clinical diagnosis between the groups, with a mean of 4.0 years across both groups from time of symptom onset to accurate diagnosis. The overall rate of incidental detection of PGL on imaging in asymptomatic patients (excluding known *SDHB*⁺ patients screened specifically for PGL) was 5.7% across both groups, although the sporadic group had a 18.8% rate of acute presentation compared with a 7.1% rate in the *SDHB*⁺ group ($P = .14$). Six of seven patients (85.7%) screened because of a known *SDHB* mutation were found to have PGL despite being asymptomatic.

Imaging findings of *SDHB*⁺ versus sporadic patients is presented in Table II. *SDHB*⁺ patients had a greater tendency to present with neoplasms above the diaphragm (16.7%) compared with the sporadic group (4.7%, $P = .11$; Fig 2). The incidence of metastatic disease was significantly higher in the *SDHB*⁺ group at 78.9% vs 48.3% in the sporadic group ($P < .001$; Fig 3). Furthermore, 38.5% of patients in the *SDHB*⁺ had either metastatic or multifocal disease (multiple primaries) at presentation compared with 16.7% in the sporadic group ($P = .012$). The overall rate of local recurrence after surgical excision was 16.2%, and the overall rate of a second primary tumor at a later date was 6.8%, with no significant difference between the groups. Median tumor volume was 50 mL in the *SDHB*⁺ group and 48 mL in the sporadic group; however, 23% of the *SDHB*⁺ patients had tumor volumes >250 mL whereas none of the genetic group had tumors this large ($P = .023$; Fig 4). Tumors in *SDHB*⁺ patients enhanced more on contrast CT, with a mean density of 108.7 HU compared with 88.4 HU in the sporadic group ($P = .014$). *SDHB*⁺ tumors were also more FDG-avid, with a mean SUV of 12.3 in the *SDHB*⁺ group compared to 8.0 in the sporadic group ($P = .027$). Using the classification of PGLs on T2-weighted MR described by Jacques et al,¹³ there was no significant difference between the groups, with 4.5% classified as type 1, 54.5% as type 2, 18.2% as type 3, and 22.7% as type 4.

DISCUSSION

As noted by Timmers et al,¹⁴ a biochemical diagnosis of PGL is typically followed by anatomic and functional imaging studies to localize the primary tumor(s) and rule out metastases. There is emerging literature concerning the sensitivity of anatomical imaging, including CT and MRI as well as functional imaging studies, including ¹⁸F-DOPA, ¹⁸F-FDG, and ¹⁸F-FDA PET, ¹²³I-MIBG scintigraphy, for the localization of PGLs, whether due to an underlying genetic mutation or in a sporadic patient. At present, however, there are few data to suggest clinical and imaging features that may distinguish sporadic from familial PGLs. We present a comparison of these features in cohorts of *SDHB*⁺ versus those with sporadic (no *SDHx*) PGL.

Clinically young age, large tumor volume, and greater rate of supra-diaphragmatic metastatic and multifocal PGLs were detected in this study in *SDHB*+ patients compared with those with sporadic PGL. These findings suggest that routine screening, including full-body imaging to detect metastatic, multifocal, and supradiaphragmatic disease is warranted in patients with known *SDHB* mutations, even in the absence of clinical signs and symptoms of catecholamine excess. Screening may begin as early as the first decade in these patients. Given the presence of large (>250 mL) tumors exclusively in *SDHB*+ in this study, it may also be of value to screen all patients with large tumor volumes (ie, >100–200 mL) for *SDHB* mutation regardless of age. At present, MR T2-signal characteristics and enhancement patterns do not appear to distinguish between these two groups of patients. Relatively greater CT enhancement and semiquantitative ¹⁸F-FDG uptake were observed in *SDHB*+ patients in this study, although further validation of these findings in larger numbers of patients is warranted in order to determine if there are thresholds specific to *SDHB*+ compared with sporadic patients that may be of diagnostic significance.

Limitations to this study include the relatively small numbers of patients studied and the limited number of patients in whom imaging of tumor was available (27 *SDHB*+ and 25 sporadic patients). Additional limitations with regard to imaging and imaging analysis include variability in CT and MRI slice thickness and timing of contrast administration, particularly when we compared studies performed nearly a decade before those performed within the past year. This study was not a randomized prospective trial that controlled rigorously for imaging protocol technique across patient cohorts over time. However, this retrospective study suggests several clinical and imaging features that may distinguish sporadic from familial PGLs. Genetic screening may be warranted in patients who present at a clinically young age, with large tumor volume, supra-diaphragmatic tumor, or metastatic or multifocal PGLs at presentation, as well as those with marked FDG uptake on ¹⁸F-FDG-PET scan. Ongoing prospective study is warranted to further validate these observations and elucidate their biological basis.

Acknowledgments

This work was supported in part by the NIH Center for Interventional Oncology and by the NIH Intramural Research Program.

References

1. DeLellis, RA.; Lloyd, RV.; Heitz, PU., et al. Pathology and Genetics: Tumours of Endocrine Organs. Oxford, UK: Oxford University Press; 2004.
2. Pacak, K.; Keiser, H.; Eisenhofer, G. Pheochromocytoma. In: De Groot, LS.; Jameson, JL., editors. Textbook of Endocrinology. 5. Philadelphia, PA: Elsevier Saunders Inc; 2005. p. 2501-34.
3. Lenders JW, Eisenhofer G, Mannelli M, et al. Pheochromocytoma. Lancet. 2005; 366:665–75. [PubMed: 16112304]
4. Baysal BE, Ferrell RE, Willett-Brozick JE, et al. Mutations in SDHD, a mitochondrial complex II gene, in hereditary paraganglioma. Science. 2000; 287:848–51. [PubMed: 10657297]
5. Astuti D, Latif F, Dallol A, et al. Gene mutations in the succinate dehydrogenase subunit SDHB cause susceptibility to familial pheochromocytoma and to familial paraganglioma. Am J Hum Genet. 2001; 69:49–54. [PubMed: 11404820]
6. Niemann S, Muller U. Mutations in SDHC cause autosomal dominant paraganglioma, type 3. Nat Genet. 2000; 26:268–70. [PubMed: 11062460]
7. Young WF Jr, Abboud AL. Editorial: paraganglioma— all in the family. J Clin Endocrinol Metab. 2006; 91:790–2. [PubMed: 16522703]
8. Timmers H, Kozupa A, Chen C, et al. Superiority of fluorodeoxyglucose positron emission tomography to other functional imaging techniques in the evaluation of metastatic SDHB-associated pheochromocytoma and paraganglioma. J Clin Oncol. 2007; 25:2262–9. [PubMed: 17538171]

9. Benn DE, Gimenez-Roqueplo AP, Reilly JR, et al. Clinical presentation and penetrance of pheochromocytoma/paraganglioma syndromes. *J Clin Endocrinol Metab.* 2006; 91:827–36. [PubMed: 16317055]
10. Neumann HP, Pawlu C, Peczkowska M, et al. Distinct clinical features of paraganglioma syndromes associated with SDHB and SDHD gene mutations. *JAMA.* 2004; 292:943–51. [PubMed: 15328326]
11. Schiavi F, Boedeker CC, Bausch B, et al. Predictors and prevalence of paraganglioma syndrome associated with mutations of the SDHC gene. *JAMA.* 2005; 294:2057–63. [PubMed: 16249420]
12. Baysal BE, Willett-Brozick JE, Lawrence EC, et al. Prevalence of SDHB, SDHC, and SDHD germline mutations in clinic patients with head and neck paragangliomas. *J Med Genet.* 2002; 39:178–83. [PubMed: 11897817]
13. Jacques A, Sahdev A, Sandrasagara M, et al. Adrenal phaeochromocytoma: correlation of MRI appearances with histology and function. *Eur Radiol.* 2005; 18:2885–92. [PubMed: 18641999]
14. Timmers H, Chen C, Carrasquillo J, et al. Comparison of 18-F-Fluoro-L-DOPA, 18F-Fluorodeoxyglucose and 18F-Fluorodopamine PET and 123I-MIBG Scintigraphy in the localization of pheochromocytoma and paraganglioma. *J Clin Endocrinol Metab.* 2009; 94:4757–67. [PubMed: 19864450]

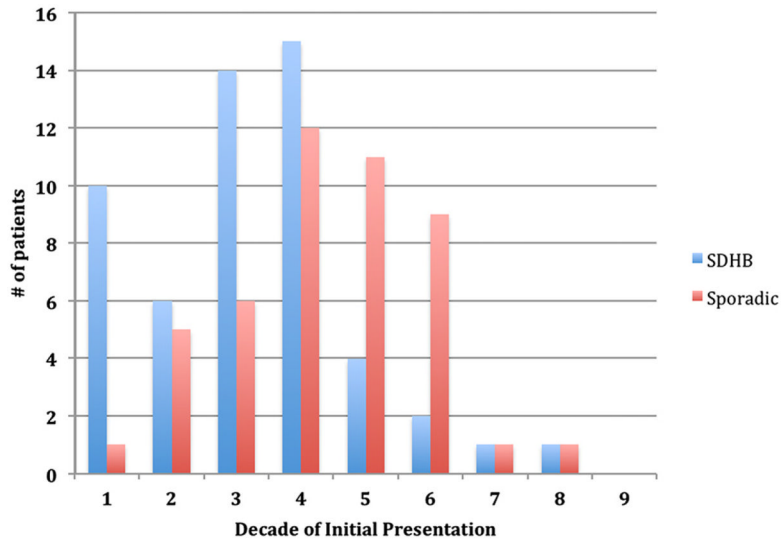


Fig. 1.

Age at diagnosis in *SDHB*+ versus sporadic patients. *SDHB*+ patients presented in the mostly first 4 decades of life, whereas patients in the sporadic group presented more in the 4th-6th decades. Time between onset of symptoms and clinical diagnosis was similar across both groups with a mean of 4.0 years.

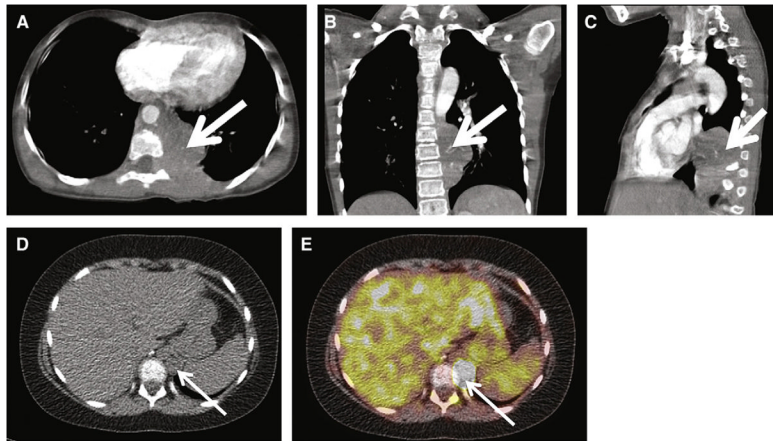


Fig. 2. Supradiaphragmatic PGL in a 9-year-old *SDHB*+ girl with a 4-year history of heat intolerance and malaise. *A–C*, Axial, coronal, and sagittal contrast-enhanced CT images, respectively, demonstrate a $5.9 \times 3.5 \times 6.1$ -cm left posterior mediastinal mass (*white arrow*). Invasion of the left T8 neural foramen is demonstrated on the axial image (*A*, *white arrowhead*). Arterial phase CT attenuation of this mass was 52 HU; portal venous phase CT attenuation of this mass was 88 HU. The patient underwent thoracotomy and resection of the posterior mediastinal mass, confirming PGL. *D–E*, at 15 months after resection, FDG PET-CT images demonstrate a new 1.5-cm retrocrural metastasis, with maximal SUV of 34 (*white arrow*) as well as pleural based masses (not shown), consistent with metastases.

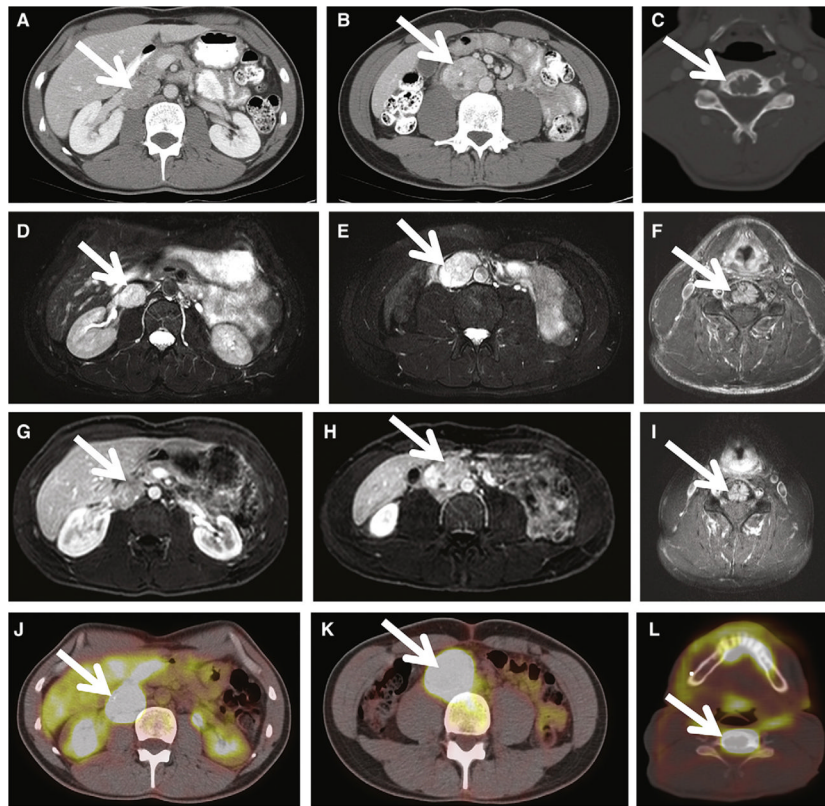


Fig. 3. Shown is a 34-year old *SDHB*+ man with history of hypertension, tachycardia, and heat intolerance with multifocal and metastatic PGLs. *A*, Axial contrast CT at the level of the renal veins demonstrates a 3-cm enhancing right renal hilar mass, consistent with extra-adrenal PGL (*white arrow*). Portal venous phase CT attenuation of this mass was 139 HU. *B*, Axial contrast CT inferior to the renal vein confluence demonstrates a 4-cm right para-aortic retroperitoneal mass (*white arrow*), consistent with PGL. Portal venous phase CT attenuation of this mass was 139 HU. *C*, Osteolytic metastasis to the C5 vertebral body (*white arrow*). *D–E*, Axial T2-weighted images demonstrate homogenous T2 hyperintensity of patient’s right retroperitoneal PGLs. T2 signal is hypointense to CSF but hyperintense to liver and spleen (group 2 classification according to criteria proposed by Jacques et al¹³). *F*, FSE T2-weighted MRI demonstrates T2 hyperintense C5 metastasis (*white arrow*). *G–I*, Axial postcontrast MRIs demonstrate enhancing right retroperitoneal PGLs and C5 metastasis, respectively (*white arrow*). *J–L*, ¹⁸F-FDG-PET CT images demonstrate hypermetabolic foci corresponding to patient’s right retroperitoneal PGLs and C5 osseous metastasis with maximal SUVs of 22, 26, and 42, respectively. The patient underwent exploratory laparotomy, resection of a right renal hilar extra-adrenal PGL, and interaortocaval extra-adrenal PGL proximal to the aortic bifurcation.

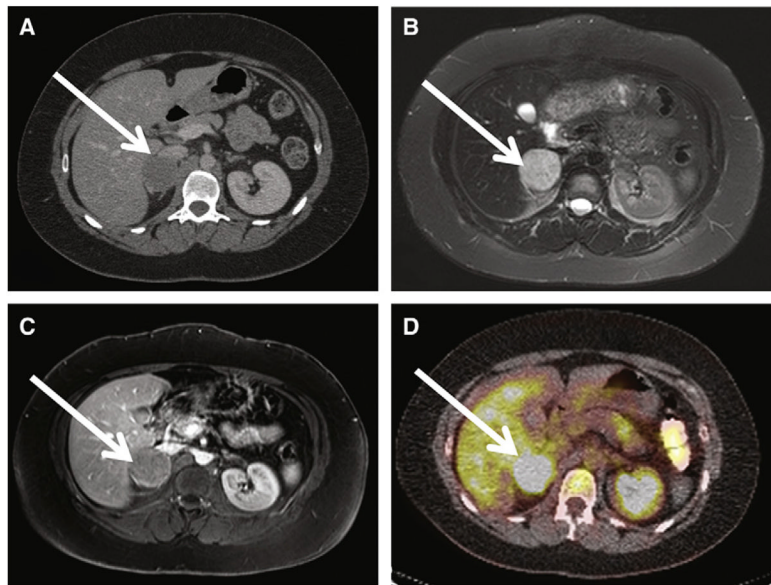


Fig. 4. Shown is a 30-year old woman with history of hypertension and headache and sporadic adrenal PGL/pheochromocytoma. *A*, Axial contrast CT at the level of the right adrenal gland demonstrates a heterogeneously enhancing $4 \times 4 \times 5$ -cm mass consistent with right adrenal PGL/pheochromocytoma (*white arrow*). Portal venous phase CT attenuation of this mass was 65 HU. *B*, Axial T2-weighted image demonstrates homogenous T2 hyperintensity of patient's right adrenal PGL. T2 signal is hypointense to CSF, but hyperintense to liver and spleen (group 2 classification according to criteria proposed by Jacques et al¹³). *C*, axial postcontrast MRIs demonstrate enhancing right adrenal PGL (*white arrow*). *D*, ¹⁸F-FDG-PET CT images demonstrate hypermetabolic focus corresponding to patient's right adrenal PGL with maximal SUV of 6. The patient underwent right laparoscopic adrenalectomy, confirming right adrenal PGL/pheochromocytoma.

Table ISummary clinical data of *SDHB*+ versus sporadic patients presenting with paraganglioma

	<i>SDHB</i> +	Sporadic
Mean age at diagnosis, yrs	28	39 *
Mean time to diagnosis, yrs	3.6 ± 4.2	4.6 ± 5.2
Acute presentation	7.1%	18.8% (<i>P</i> = .14)
Incidental detection	5.4%	6.3%
Metastatic/multifocal at presentation	38.5%	16.7% *
Overall rate of metastatic disease	78.9%	48.3% *
Local recurrence after resection	12.3%	20%
Secondary PGL	7.0%	6.7%

* Indicates statistically significant difference between groups (*P* < .05). Overall, *SDHB*+ patients presented at a younger age and were more likely to present with and develop metastatic or multifocal disease.

PGL, Paraganglioma; *SDHB*+, succinate dehydrogenase positive.

Table IISummary imaging findings of *SDHB*+ versus sporadic patients presenting with

	SDHB+	Sporadic
Supradiaphragmatic neoplasms	16.7%	4.7% ($P = .11$)
Median tumor volume, mL	48	50
Tumors >250 mL	23%	0%*
Mean CT density, HU	108.7	88.4*
Mean ^{18}F -FDG uptake, SUV	12.3	8.0*
Lesion appearance on T2W MRI		
Group 1	5%	4%
Group 2	57%	52%
Group 3	19%	17%
Group 4	19%	26%

* Indicates statistically significant difference between groups ($P < .05$). *SDHB*+ patients had greater rates of supradiaphragmatic neoplasms, a greater incidence of large tumors (>250 mL), and a greater mean CT density and SUV uptake on ^{18}F -FDG-PET. There were no differences in T2W MRI characteristics as categorized by Jacques et al.¹³

CT, Computed tomography; *^{18}F -FDG*, ^{18}F -fluoro-deoxy-glucose; *HU*, Hounsfield units; *MRI*, magnetic resonance imaging; *PET*, positron emission tomography; *T2W*, T2-weighted; *SDHB*+, succinate dehydrogenase positive; *SUV*, standardized uptake value.